

Original article

Novel 5,7-disubstituted 6-amino-5H-pyrrolo [3,2-b]pyrazine-2,3-dicarbonitriles, the promising protein kinase inhibitors with antiproliferative activity

G.G. Dubinina^{*}, M.O. Platonov, S.M. Golovach, P.O. Borysko
A.O. Tolmachov, Y.M. Volovenko

ChemBio Center, Kiev National University, 6 Sosury Street, 02090 Kiev, Ukraine

Received in revised form 13 March 2006; accepted 14 March 2006

Available online 03 May 2006

Abstract

New derivatives of pyrrolo[2,3-b]pyrazine were synthesized and tested on a panel of cultured human tumor cell lines. It was found that 6-amino-5-(3-chlorophenylamino)-7-(1-methyl-1H-benzo[d]imidazol-2-yl)-5H-pyrrolo[3,2-b]pyrazine-2,3-dicarbonitrile (**4j**) exhibited a significant antiproliferative activity: GI50 for cell lines RXF 393 (renal cancer) and BT-549 (breast cancer) were 14 and 82 nM, respectively. To identify possible molecular targets, docking of the most active compounds into the active sites of cyclin-dependent kinases was performed. Molecular modeling of the inhibitor–enzyme complexes showed the differences in the binding poses of new pyrrolo[2,3-b]pyrazine derivatives in the kinase ATP-binding site compared with known pyrrolo[2,3-b]pyrazine inhibitors called aloisines. The patterns of drug kinase interactions correlated well with antiproliferative activities of novel derivatives. Key interactions and binding mode of docked compounds are discussed.

© 2006 Elsevier SAS. All rights reserved.

Keywords: Antiproliferative agents; Cytostatic agents; Pyrrolo[2,3-b]pyrazine; Kinase inhibitor; Molecular modeling; Docking

1. Introduction

The derivatives of pyrrolo[2,3-b]pyrazine are known to be biologically active. In addition to having antibronchospastic effect [1] and the ability to inhibit the activity of p38 MAP kinase [2], the compounds of this class can also inhibit cyclin-dependent kinases (CDKs) and glycogen synthase kinase-3 (GSK-3), thereby exerting an antiproliferative effect [3–6]. The most efficient pyrrolo[2,3-b]pyrazine derivatives are aloisines. Fig. 1 shows the structures of aloisines A and B.

Abbreviations: CDK, cyclin-dependent kinase; EGFR, epidermal growth factor receptor kinase; GI₅₀, growth inhibition; GSK-3, glycogen synthase kinase-3; LC₅₀, lethal concentration; LC/MS, liquid chromatography/mass spectrometry; MAP, mitogen activated protein kinase; PG, percentage growth; RMSD, root mean square deviation; SAR, structure–activity relationship; SRB, sulforhodamine B; TGI, total growth inhibition; *t*_R, retention time.

^{*} Corresponding author. Tel.: +380 44 206 4579; fax: +380 44 537 3253.

E-mail address: g.dubinina@univ.kiev.ua (G.G. Dubinina).

Aloisines bind to the kinase ATP-binding pocket as competitive inhibitors [4,6]. The structures of the active sites and interaction patterns of the kinases with aloisine A and B (aloisine B-CDK2 and aloisine A-CDK5 (1ung.pdb) complexes; [4]) have been investigated by the X-ray method. The authors found that the key interactions were the two hydrogen bonds with the backbone nitrogen and oxygen atoms of Leu 83 (CDK2) and Cys83 (CDK5) formed by the nitrogen atom in position 4 and the hydrogen atom adjacent to N(5) of the pyrrolo[2,3-b]pyrazine cycle. The third hydrogen bond was formed between the nitrogen atom N(1) and ϵ -amino group of Lys33 (aloisine B/CDK2) [4] and the nitrogen N(1) of aloisine A was engaged in an hydrogen bonding network involving the side chains of Lys33, Glu51, Asn144, and two water molecules (CDK5) [6]. Structure–activity relationship (SAR) studies of 50 aloisine derivatives with different substituents in the positions **2**, **3**, **7a–e** (Fig. 1) were performed [4]. The replacement by carbon atom or an alkylation of any of the nitrogen atoms that formed the essential hydrogen bonds dramatically de-

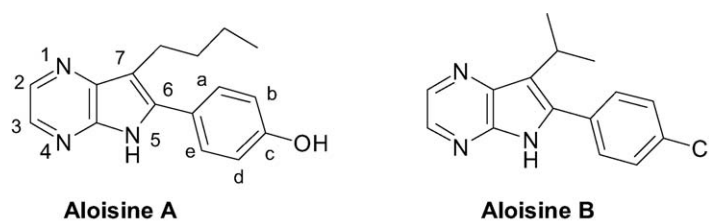


Fig. 1. Aloisine A and B, the inhibitors of CDKs and GSK-3.

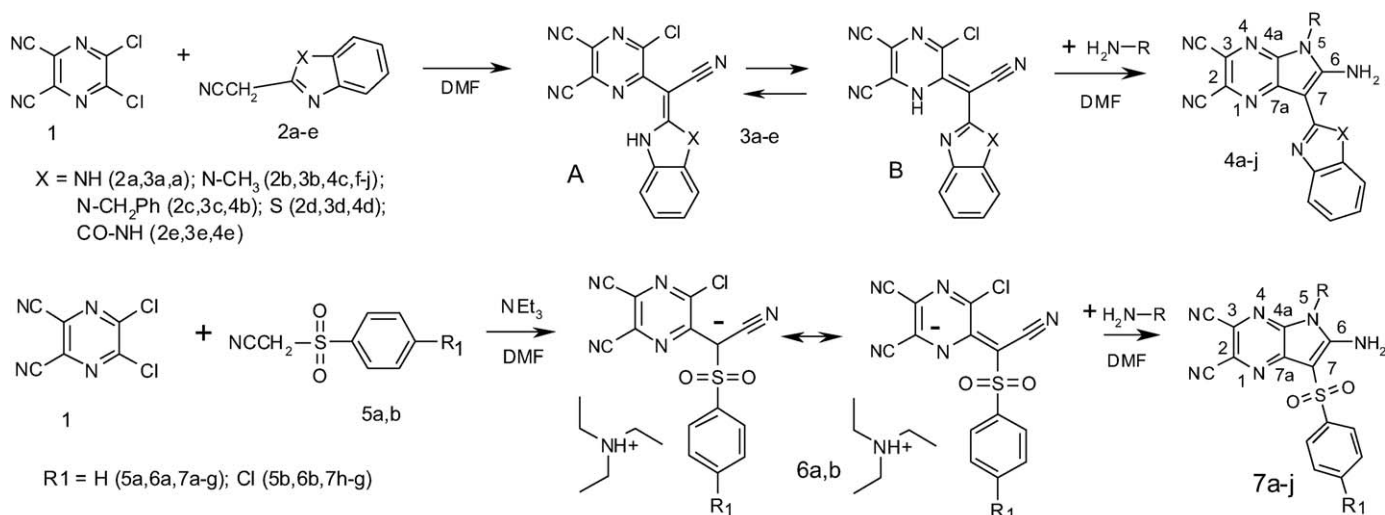
creased the inhibitory activity. Introducing one, two, three methoxy groups at the positions **a–d** of the phenyl ring or its replacement by five or six membered heterocycles and the presence of any substituents at the position 2,3 of pyrrolo[2,3-*b*]pyrazine cycle decreased the inhibitory activity. In contrast, the presence of alkyl substituent at the position 7 and chlorine atom or hydroxy group at the **c**-position of the phenyl ring increased the anti-enzymatic effect. These facts correlated well with X-ray data on interaction of these groups with the side chains and hydrophobic pockets of the binding sites [4,6].

2. Chemistry

In this work, 20 new pyrrolo[2,3-*b*]pyrazine derivatives were synthesized, namely, 5,7-disubstituted 6-aminopyrrolo[2,3-*b*]pyrazine-2,3-dicarbonitriles **4a–j**, **7a–j** (Scheme 1). A two-stage nucleophilic substitution of chlorine atoms in 5,6-dichloropyrazine-2,3-dicarbonitrile **1** with C- and N-nucleophiles was used for building the pyrrolo[2,3-*b*]pyrazine cycle (Scheme 1). α -Azaheteroarylacetonitriles **2a–e** and 2-(phenylsulfonyl)acetonitriles **5a, b** were used in the first step as C-nucleophiles (Scheme 1) to produce **3a–e** and **6a, b**. These products can exist in two tautomeric forms, A and B [7]. The next step was the nucleophilic substitution of the second chlorine atom by N-nucleophiles, primary amines and 3-chlorophenylhydrazine (for compound **4j**), followed by the addition of the secondary amine to nitrile group and formation of the pyrrolo[2,3-*b*]pyrazine cycle. Compounds **4a–e** were synthesized as

described earlier in [7], and the derivatives **4f–j** were obtained. Compounds **6a, b** were synthesized as salts presented by two resonance structures, where the negative charge is delocalized between the carbon atom of the acetonitrile moiety and the nitrogen atom of the pyrazine ring. The salt formation can be explained by high C–H acidity of the carbon atom that has three electron-withdrawing groups. Thus, a strong C–H acid and hydrochloric acid were formed in this reaction. These acids competitively protonated triethylamine (TEA) used as a base. Due to this reason, the highest yields were obtained with 2 equiv. of TEA. In the previous study we investigated the formation of a salt product in the reaction of 5,6-dichloropyrazine-2,3-dicarbonitrile with malononitrile and TEA as a base, and found that the C–H acid with $pK_a = 0.84$ was obtained [8]. The interaction of compounds **6a, b** with primary amines formed pyrrolo[2,3-*b*]pyrazine **7a–j**.

^1H NMR spectra of compounds **4a–j**, **7a–j** showed a singlet of the amino group protons at 8.21–9.85 ppm (s, 2H, NH_2) that disappeared after the addition of D_2O . Singlets of the labile protons of compounds **3a–e** at 12.58–12.76 ppm were absent in the spectra of compounds **4a–j**, and multiplet signals of $\text{H-N}^+(\text{Et})_3$ of compounds **6a, b** at 10.74–11.20 ppm were absent in the spectra of products **7a–j**. In compounds **3a–e**, **6a, b** the characteristic strong band of the conjugated nitrile group of the acetonitrile moiety was observed in IR spectra ($2195\text{--}2185\text{ cm}^{-1}$). This band was not present in the IR spectra of products **4a–j**, **7a–j**. Low intensity bands of pyrazine nitrile bonds were observed in the $2227\text{--}2210\text{ cm}^{-1}$ range.



Scheme 1.

3. Antiproliferative activity studies

The antiproliferative activity of novel compounds was investigated in National Cancer Institute, USA (Developmental Therapeutics Program). First, a pre-screening was performed using MCF-7 (breast cancer), NCI-H460 (non-small cell lung cancer) and SF-268 (glioma) cell lines; all compounds were tested at 100 μ M concentration. Compounds that demonstrated antiproliferative activity $\geq 68\%$ were selected for advanced testing in a panel of 60 cancer cell lines at five concentrations that differed 10-fold (from 10 nM to 100 μ M).

4. In silico analysis

Molecular modeling based on docking approach was used to find possible target(s) of the antiproliferative activity. Docking of new pyrrolo[2,3-b]pyrazine derivatives into the active sites of CDK2, CDK5, GSK-3 and EGFR was performed. To estimate the binding of synthesized compounds to the active sites of these kinases and to tune docking parameters, we investigated the known X-ray ligand–kinase complexes and created a training set of known inhibitors for each kinase. The docking of known aloisine analogs and SAR information [4] were used for scoring function selection for estimation of ligand-CDK2, 5 and GSK-3 complexes. An in-house software package, Multi-Filter, was used for geometric filtration. The main idea behind geometry filters was based on the fact that molecular docking (Flo+, QXP) can predict the molecular geometric stationary point with sufficient accuracy [9], proved by a number of X-ray structural analyses. Other characteristics, such as energy, sometimes cannot be calculated with sufficient precision by the force-field method because force-field approximations do not take into account some important factors, e.g. specific properties of the charge density distribution. The main purpose of geometry filtering was to define the compounds that fit the binding pocket, meaning an efficient ligand–receptor interaction (high affinity). The selected compounds had the best fitting in the active site and the lowest values for the steric and chemical repulsive interactions with the receptor. The contact and hydrogen bond energy values (pI , Cntc, Hbnd) were used as additional filtering parameters (Tables 3 and 4).

5. Results and discussion

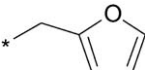
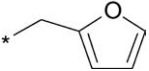
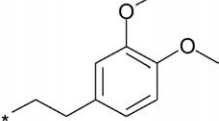
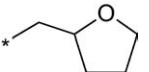
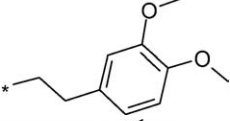
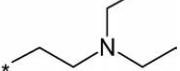
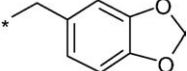
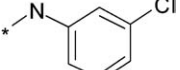
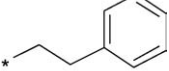
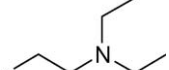
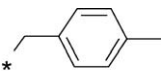
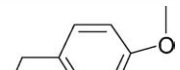
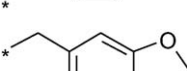
Seventeen newly synthesized compounds **4**, **7** (Table 1) were tested for growth inhibitory activity against human cancer cell lines (in collaboration with National Cancer Institute). Compounds **4f–h**, **j** and **7d**, **j** that demonstrated antiproliferative activity $\geq 68\%$ at a drug concentration of 100 nM were selected for advanced testing in a panel of 60 cancer cell lines at five concentrations that differed 10-fold (from 10 nM to 100 μ M). Table 2 shows the data on compounds that suppressed cell proliferation at nanomolar concentrations (a 50% growth inhibition $GI_{50} < 1 \mu$ M).

It was found that compound **4j** displayed a significant antiproliferative activity: GI_{50} s for cell lines RXF 393 (renal can-

cer) and BT-549 (breast cancer) were 14 and 82 nM, respectively. Compound **7j** showed selective activity against HCC-2998 cell line, while its potency for other lines was negligible. The GI_{50} and LC_{50} values for compound **4j** differed by a factor of ~ 2430 . The SAR analysis of substituents at position 5 of pyrrolo[2,3-b]pyrazine cycle showed that the addition of one carbon atom at this position from benzyl to phenethyl moiety (Table 1, compounds **4c**, **e**; **7a**, **i**) decreased the antiproliferative activity. Introducing methoxy groups (**4c**, **e**; **7e**) or methylenedioxy moiety (**4i**, **7f**) to the phenyl ring of the substituent at position 5, or replacing the phenyl ring by oxygen containing ring (furan **4a**, **b**, tetrahydrofuran **4d**), resulted in the loss of the activity. However, the presence of hydrophobic halogen atom in the *m,p*-position of phenyl ring at position 5 of pyrrolo[2,3-b]pyrazine cycle (compounds **4g**, **h**, **j**; **7d**, **j**) increased the antiproliferative efficacy.

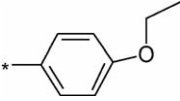
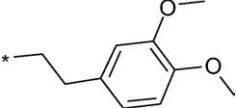
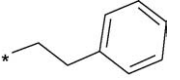
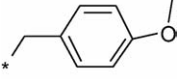
To identify possible targets, docking of the synthesized compounds into the active sites of CDK2, CDK5, GSK-3 and epidermal growth factor receptor (EGFR) kinases was performed. Docking of known aloisine analogs and SAR information [4] were used as a training set to select a scoring function for estimating the interactions of new pyrrolo[2,3-b]pyrazine derivatives with the binding sites of these kinases. The main affinity criterion was the presence of two hydrogen bonds formed by the ligand with Glu81 and Cys83 amino acid residues of CDK5 in the ligand–receptor complex. The 2.5 Å distance was assumed as the largest possible distance for hydrogen bond formation. The aloisine A/CDK5 complex (1ung.pdb) [6] was investigated to identify the key points of interaction. Fifty-one aloisine derivatives in the tested set were docked to the CDK5 site model. Filtering criteria were developed based on the activity data of the investigated aloisines [4] (Table 3). Next, docking of 51 aloisines to GSK-3 (1UV5) [10] was performed and the same trends were observed. Similarly to CDK5, the formation of two hydrogen bonds involving Asp133 and Val135 was critical for efficient GSK-3 binding as ATP-competitive inhibitors. To obtain the geometry and energy filtering criteria, the complexes of CDK2 (1AQ1) [11] and EGFR (1M17) [12] were analyzed and docked using a set of known inhibitors of different chemical classes [5,13–15]. Similar to CDK5 and GSK-3, it was found that two hydrogen bonds were necessary for high calculated affinity. The bonds were formed between the Glu81 and Leu83 amino acid residues for CDK2, and between Ser766 and Gln767 for EGFR. These patterns may be used as hinge region-directed filters for ATP-competitive inhibitor searching. Nevertheless, the general geometric filters which were applied for post-docking inhibitor selection were not so rigid: one distance was 5.5 Å from any atom of ligand to the marked atom deep inside the receptor pocket and the second distance was 2.5 Å from the corresponded above amino acid residues (Table 3). Compounds not satisfying the requirements of the geometric filters were classified as non-active (Table 4). The calculated energy scoring functions for the rest of compounds which were passed through geometric filters successfully, were compared with such calculated parameters of the training sets of the known

Table 1
Antiproliferative activity of compounds 4a–j, 7a–j

Compounds	Substituents		Antiproliferative activity (%) at 100 μ M of tested compounds*			Selected for further studies ^a
	X; R ₁	R	Breast cancer MCF-7	lung cancer NCI-H460	CNS tumor SF-268	
4a [7]	X = NH		9	30	1	No
4b [7]	X = N-CH ₂ Ph		25	31	8	No
4c [7]	X = N-CH ₃		-2	-1	-31	No
4d [7]	X = S		5	11	-21	No
4e [7]	X = CONH		29	-7	-6	No
4f	X = N-CH ₃		74	94	11	Yes
4g	X = N-CH ₃		67	74	-4	Yes
4h	X = N-CH ₃		55	83	-10	Yes
4i	X = N-CH ₃		36	9	-13	No
4j	X = N-CH ₃		82	87	55	Yes
7a	R ₁ = H		40	54	18	No
7b	R ₁ = H		43	42	12	No
7c	R ₁ = H		ND	ND	ND	
7d	R ₁ = H		31	83	-1	Yes
7e	R ₁ = H		16	36	2	No
7f	R ₁ = H		14	34	0	No

(continued)

Table 1 (continued)

Compounds	X; R ₁	Substituents R	Antiproliferative activity (%) at 100 μM of tested compounds*			Selected for further studies ^a
			Breast cancer MCF-7	lung cancer NCI-H460	CNS tumor SF-268	
7g	R ₁ = H		ND	ND	ND	
7h	R ₁ = Cl		ND	ND	ND	
7i	R ₁ = Cl		11	14	-12	No
7j	R ₁ = Cl		31	85	6	Yes

^a Negative value of antiproliferative activity (%) means that the tested compound stimulated cell growth in comparison with control.

inhibitors (with $IC_{50} < 50$ μM) (Tables 3 and 4). It was revealed, that the most promising among potential inhibitors were compounds **7b**, **j** (CDK2); **4f**, **j** (CDK5); **7d**, **j** (GSK-3); **4h**, **7i** (EGFR) which formed high energy hydrogen bonds preferably with hinge region. Unfortunately, neither of the modern docking programs is able to predict the real affinity of the compounds with high percent of the hitting. However, the application of the structure-based approach may be very useful for the definition of the binding poses and further directed modification of the active molecules.

Thus, our novel antiproliferative agents, pyrrolo[2,3-*b*]pyrazine derivatives **4a–j**, **7a–j** were docked in the binding sites of kinases CDK2, CDK5, GSK-3 and EGFR. The above filtering criteria were applied (Tables 3 and 4). The essential aloisine hydrogen bonds in the binding sites were formed by the nitrogen atom at position N(4) and the hydrogen atom at N(5) (described by Standard Kinase Interaction Pattern (Fig. 2)) [16]. This binding pattern summarizes the majority of known kinase inhibitor binding modes due to the conservative interactions of ATP-competitive inhibitors and common features of kinase binding sites. In our docking studies the orientation of compounds depended primarily on the substituents at the positions 2,3,5,7 of the pyrrolo[2,3-*b*]pyrazine cycle. The presence of nitrile groups and a substituent at the position 5 changed the binding mode significantly in comparison with aloisine (Fig. 2). This can be explained by the fact that the crucial hydrogen bonds for 6-aminopyrrolo[2,3-*b*]pyrazine-2,3-dicarbonitriles **4a–j**, **7a–j** were formed by the amino group and the oxygen atom of the sulfo group or by the heterocyclic nitrogen atom at the position 7, due to conformational reasons. In addition, being smaller than compounds **4**, **7**, aloisine does not fill the hydrophobic pocket of the kinase active site (Fig. 2).

Analysis of 6-amino-5-(3-chlorophenylamino)-7-(1-methyl-1H-benzo[d]imidazol-2-yl)-5H-pyrrolo[3,2-*b*]pyrazine-2,3-dicarbonitrile (**4j**)—CDK2 complex showed that hydrogen bonds were not formed, nor was the conformation of the inhibitor

planar. In contrast, for GSK-3 the two hydrogen bonds were formed by the amino group at the position 6. The interaction of compound **4j** with CDK5 was found to have high binding energy of 74.0 kJ mol⁻¹ (Table 4). Spatial models of the inhibitor **4j** were almost planar, and the benzoimidazole ring efficiently interacted with the hydrophobic pocket, providing an additional stability to the complex. Also, three hydrogen bonds were formed in the **4j**-CDK5 complex (Fig. 3).

The amino group interacted with Cys83 and Asp84 amino residues forming two bonds. An additional hydrogen bond was formed between Cys83 and the hydrogen atom of the secondary amine moiety at the position 5 of the pyrrolo[2,3-*b*]pyrazine cycle. The hydrophobic interaction was observed between the chlorine atom and the phenyl ring of the Phe80 amino residue (bond length 3.82 Å). Such hydrophobic interaction was observed for compounds that had a halogen atom in the *m,p*-position of phenyl ring at position 5 of pyrrolo[2,3-*b*]pyrazine cycle (compounds **4g**, **h**, **j**; **7d**, **j**). Addition of one carbon atom at position 5 from benzyl to phenethyl moiety (Table 1, compounds **4c**, **e**; **7a**, **i**) led to the steric clashes in the hydrophobic pocket of kinases. Thus, the energy of the ligand conformation was high and, as a result, the affinity of the ligand decreased. These patterns correlated well with antiproliferative activities of the tested compounds as discussed above (Tables 1 and 2).

The best binding interactions for 6-amino-5-(4-methoxybenzyl)-7-(4-chlorophenylsulfonyl)-5H-pyrrolo[3,2-*b*]pyrazine-2,3-dicarbonitrile (**7j**) were formed in the complex with CDK2 (Fig. 4) and GSK-3. The oxygen atom of the sulfo group in CDK2 formed a hydrogen bond with the H–N of the Leu83 residue (bond length 2.7 Å), while the oxygen atom of the methoxy group bound to Asp145 (1.82 Å). The stacking interaction was observed between the phenyl ring of the benzyl moiety and the phenyl ring of the Phe80 residue (bond length 3.56 Å). An additional hydrophobic interaction was found between the chlorine atom and the phenyl ring of the Phe82 amino residue (3.65 Å).

Table 2
Antiproliferative activity of pyrrolo[2,3-b]pyrazines **4f–h, j**; **7d, j** against selected human cancer cell lines

Cell lines	Parameters ^a	Concentration (μM)					
		4f	4g	4h	4j	7d	7j
HOP-92 (non-small cell lung cancer)	GI ₅₀	0.71	1.63	2.35	16.5	12.3	11.5
	TGI	3.47	18.4	10.1	>50	46.2	>50
	LC ₅₀	28.5	>50	35.8	>50	>50	>50
NCI-H322M (non-small cell lung cancer)	GI ₅₀	1.01	0.62	ND ^b	9.62	9.99	ND
	TGI	6.17	4.87		20.4	28.9	
	LC ₅₀	> 50	> 50		43.2	> 50	
EKVX (non-small cell lung cancer)	GI ₅₀	7.22	4.16	7.04	0.84	19.1	> 50
	TGI	20.3	> 50	46.1	7.45	> 50	> 50
	LC ₅₀	> 50	> 50	> 50	45.5	> 50	> 50
UACC-257 (melanoma)	GI ₅₀	0.66	4.51	13.5	6.18	33.1	> 50
	TGI	4.24	> 50	> 50	15.9	> 50	> 50
	LC ₅₀	28.0	> 50	> 50	40.7	> 50	> 50
LOX IMVI (melanoma)	GI ₅₀	1.86	0.74	1.14	5.25	0.93	8.26
	TGI	5.06	2.18	5.67	11.5	4.17	38.3
	LC ₅₀	49.1	11.0	36.9	25.1	19.5	> 50
PC-3 (prostate cancer)	GI ₅₀	0.31	2.61	4.62	10.5	18.3	33.5
	TGI	7.58	> 50	> 50	33.9	> 50	> 50
	LC ₅₀	50.0	> 50	> 50	> 50	> 50	> 50
IGROV1 (ovarian cancer)	GI ₅₀	2.68	0.89	1.54	1.27	9.65	21.6
	TGI	20.7	ND	7.71	12.6	42.3	> 50
	LC ₅₀	> 50	> 50	> 50	> 50	> 50	> 50
OVCAR-3 (ovarian cancer)	GI ₅₀	1.66	0.84	1.37	6.96	12.0	2.90
	TGI	8.64	2.60	6.20	33.5	>50	19.4
	LC ₅₀	49.2	20.7	30.7	>50	>50	> 50
786-0 (renal cancer)	GI ₅₀	1.40	0.92	7.69	8.91	7.08	3.33
	TGI	4.38	3.59	17.4	37.3	15.6	> 50
	LC ₅₀	36.7	> 50	39.5	> 50	34.3	> 50
ACHN (renal cancer)	GI ₅₀	0.70	0.83	1.50	5.44	4.23	6.22
	TGI	1.53	2.43	6.38	15.0	13.0	>50
	LC ₅₀	33.8	10.5	22.1	41.2	35.1	>50
RXF 393 (renal cancer)	GI ₅₀	1.98	1.70	0.57	0.014	2.45	1.45
	TGI	4.46	4.86	4.67	3.54	13.9	5.37
	LC ₅₀	> 50	> 50	21.9	34.0	> 50	> 50
BT-549 (breast cancer)	GI ₅₀	9.56	2.79	6.44	0.082	10.8	34.3
	TGI	24.3	18.2	15.6	1.96	41.7	> 50
	LC ₅₀	> 50	> 50	38.0	26.0	> 50	> 50
NCI/ADR-RES (breast cancer)	GI ₅₀	10.2	7.56	2.36	0.84	0.42	1.15
	TGI	34.7	22.5	10.8	14.1	10.3	6.00
	LC ₅₀	> 50	> 50	41.2	> 50	26.6	20.0
HCC-2998 (colon cancer)	GI ₅₀	0.70	1.35	1.08	6.95	3.60	0.55
	TGI	1.41	3.05	3.57	16.9	10.8	1.54
	LC ₅₀	28.5	12.6	13.1	40.9	25.6	ND

^a GI₅₀ – concentration of compound sufficient to reduce the number of viable cells by 50%; TGI – concentration of compound that completely suppressed cell growth; LC₅₀ – concentration of compound that caused death of 50% of cancer cells.

^b ND, not determined.

Table 3
Geometric filters and calculated energy scoring functions (QXP/FLO+) for training set of known inhibitors

Kinase target	PDB code	Geometric filters			Calculated energy scoring functions* (QXP/FLO+) for the training set of known inhibitors			Source for training set
		Amino acid residue	Marked atom	Distance (Å)	pI	Cntc	Hbnd	
CDK2	1AQ1	Phe80	C (meta-position of the phenyl ring)	5.5	3.9 ÷ 5.2	-59.0 ÷	-2.1 ÷ -3.0	[5,13–15]
		Leu83	O (C = O group)	2.5		-78.0		
CDK5	1UNG	Phe80	C (meta-position)	5.5	3.4 ÷ 4.9	-46.1 ÷	-0.1 ÷ -2.3	[4]
		Cys83	N	2.5		-64.4		
GSK-3	1UV5	Leu132	C (methyl group)	5.5	4.4 ÷ 5.0	-54.5 ÷	-3.1 ÷ -3.5	[4]
		Val135	N	2.5		-60.3		
EGFR	1M17	Thr766	C (methyl group)	5.5	3.2 ÷ 5.4	-40.0 ÷	-3.1 ÷ -4.0	[5,13–15]
		Met769	N	2.5		-75.4		

* pI, kJ mol⁻¹ (pI = -log₁₀(Ki)); Cntc, kJ (ligand-site contact energy + site entropy); Hbnd, kJ (hydrogen bond energy).

Table 4
The energy scoring functions (QXP/FLO+) for compounds which passed through geometric filtration

Compounds	Calculated energy scoring functions (QXP/FLO+)*											
	CDK2			CDK5			GSK-3			EGFR		
	pI	Cntc	Hbnd	pI	Cntc	Hbnd	pI	Cntc	Hbnd	pI	Cntc	Hbnd
4a	5.1	-62.3	-0.1	4.7	-63.0	-4.1	5.3	-64.4	-2.3	-	-	-
4b	-	-	-	-	-	-	-	-	-	-	-	-
4c	-	-	-	-	-	-	-	-	-	4.2	-70.2	-1.1
4d	-	-	-	4.4	-70.4	-3.0	-	-	-	-	-	-
4e	-	-	-	-	-	-	-	-	-	3.8	-69.8	-1.7
4f	-	-	-	4.8	-75.1	-9.2	-	-	-	-	-	-
4g	4.5	-71.9	-0.1	-	-	-	-	-	-	-	-	-
4h	-	-	-	-	-	-	-	-	-	4.7	-64.4	-2.1
4i	-	-	-	-	-	-	-	-	-	-	-	-
4j	5.6	-60.5	-0.2	5.4	-74.0	-4.6	5.7	-65.5	-0.8	-	-	-
7a	-	-	-	4.4	-78.4	-3.8	-	-	-	3.9	-73.7	-0.2
7b	3.1	-67.6	-5.9	-	-	-	-	-	-	-	-	-
7c	-	-	-	-	-	-	-	-	-	4.0	-62.7	-1.1
7d	4.6	-71.3	0.0	3.8	-69.6	-3.7	4.4	-73.1	-2.9	-	-	-
7e	4.0	-75.2	-0.1	-	-	-	-	-	-	-	-	-
7f	-	-	-	-	-	-	4.7	-82.3	-2.5	4.0	-63.3	-0.1
7g	-	-	-	4.3	-72.8	-2.3	-	-	-	-	-	-
7h	-	-	-	-	-	-	-	-	-	-	-	-
7i	4.1	-65.1	-0.1	-	-	-	-	-	-	3.6	-62.8	-1.8
7j	5.0	-84.6	-3.1	-	-	-	5.1	-76.3	-2.9	-	-	-

* “-” indicates that compound is discarded as non-active after geometric filtration.

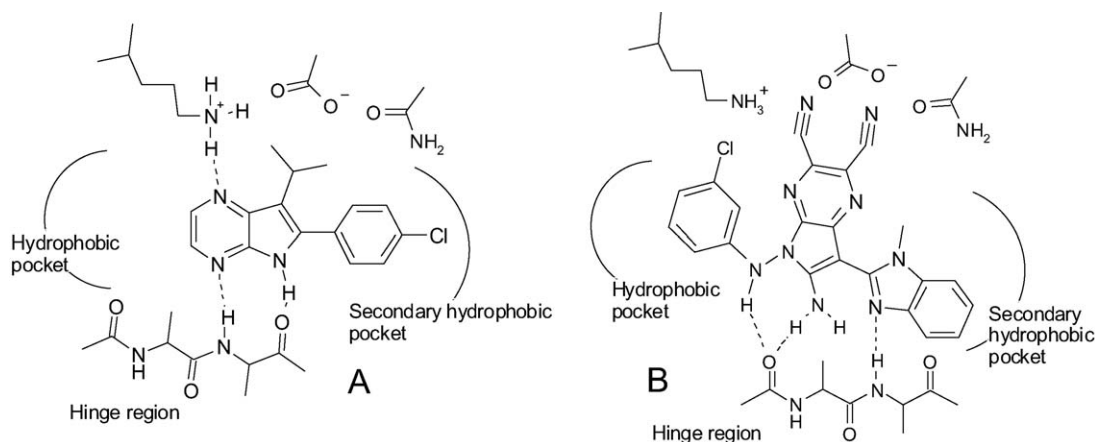


Fig. 2. Schematic representation of the binding mode of the **aloisine B** (A) and compound **4j** (B) by the Standard Kinase Interaction Pattern [16].

6. Conclusions

Altogether, our data demonstrate that 5,7-disubstituted 6-aminopyrrolo[2,3-b]pyrazine-2,3-dicarbonitriles possess the antiproliferative properties for human cancer cell lines (Tables 1 and 2) and can be considered as potential protein kinase inhibitors. The most promising targets for this class of compounds were CDK5 and GSK-3 based on higher scoring functions and geometric criteria for the calculated complexes of pyrrolo[2,3-b]pyrazine derivatives with these targets including the number of the formed H-bonds (Tables 3 and 4). Presumably, this observation can be related to the fact that the binding sites of CDK5 and GSK-3 are larger and more flexible compared to the sites of other kinases. It was found, that the most potential promising inhibitors for each target were compounds **7b**, **j** (CDK2); **4f**, **j** (CDK5); **7d**, **j** (GSK-3); **4h**, **7i** (EGFR). Molecular modeling of the inhibitor–enzyme complexes showed the

differences in the binding pose of these compounds in the kinase ATP-binding site in comparison with aloisines (Figs. 2–4). Introducing the anilino moiety into the position 5 of pyrrolo[2,3-b]pyrazine cycle (compound **4j**; Tables 1 and 2 and Figs. 2 and 3) by reaction with 3-chlorophenylhydrazine increased the antiproliferative activity. The increased energy of binding and formation of an additional hydrogen bond were observed for GSK-3 and CDK-5. This fact and structure–antiproliferative activity analysis of other substituents at the 5 and 7 position of the pyrrolo[2,3-b]pyrazine cycle correlates well with the calculated binding poses as discussed above and opens new possibilities for further purposeful modification of substituents at 5 position of 6-aminopyrrolo[2,3-b]pyrazine-2,3-dicarbonitriles. High selectivity of interaction of the compounds **4f–h**, **j**; **7d**, **j** with their particular targets may be a reason for the dramatic difference between GI_{50} and LC_{50} (Table 2, compound **4j**). Although more studies are needed to evaluate the potency of

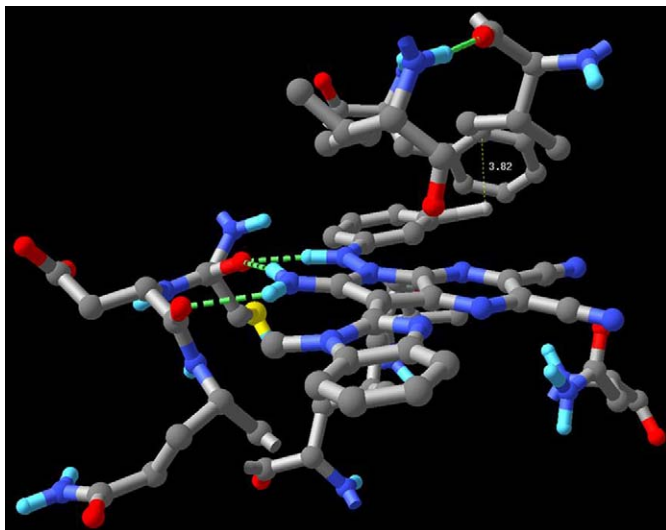


Fig. 3. The CDK5-4 j complex (QXP/FLO+ docking software).

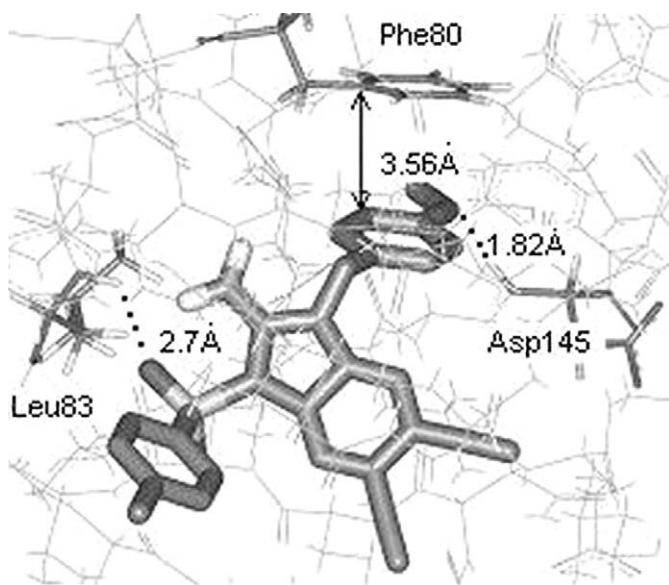


Fig. 4. The CDK2-7 j complex (QXP/FLO+ docking software).

these compounds to non-malignant tissues, the 5,7-disubstituted 6-aminopyrrolo[2,3-b]pyrazine-2,3-dicarbonitriles are promising as cytostatic agents with little or no general toxicity.

7. Experimental protocols

Antiproliferative activity assay was carried out jointly with the US National Cancer Institute according to Developmental Therapeutics Program. Sixty human cancer cell lines were used to determine the in vitro anticancer activity of the tested compounds. The anticancer assay was based on the protein staining using sulforhodamine B (SRB). The calculated measure of efficiency was percentage growth (PG). The effect of the compound on the cell line was calculated from the change in the optical density values of SRB-derived coloration observed before the exposure of the cells to the tested compounds and 48 hours after exposure, and, for the baseline cell

culture, after a 48 hour delay without any exposure. The response parameters GI_{50} , TGI, LC_{50} are interpolated values representing the concentrations at which PG was +50, 0 and –50, respectively.

Docking procedure. All docking procedures were performed with QXP/Flo+ program developed by McMartin and Bohacek [17]. Docking with flexible ligand and rigid protein site using systematic docking algorithm (SDOCK+) was employed, as it yielded good correlation of the energy parameters and X-ray RMSD on the training set of compounds. The maximal number of search iterations (search step number) was 250 steps. The best (five) complexes (saved docking poses) were used for final post-docking filtration for each compound. Intrinsic QXP scoring functions (pI , Cntc, hbnd) and two distances from essential atoms (in-house software package, Multi-Filter) were applied for energetic and geometric filtration, respectively. The minimal geometric criteria for the post-docking selection based on calculated parameters of the training sets are shown in the Table 3. Compounds which did not satisfy the requirements of the geometric filters were discarded as non-active (Table 4). The training sets of known inhibitors were scored and ranked after the docking procedure in the respective kinases and the range of the scoring functions was obtained and applied for the new inhibitor selection. There are intrinsic scoring functions (QXP/FLO+) for the compounds which have passed successfully through geometric filters, shown in Table 4.

Identification of structures and purity tests. Structure and purity of synthesized compounds were verified by IR spectra recorded on UR-20, Specord 75-I and Pye Unicam, LC/MS (Agilent LC/MSD SL and VL mass spectrometers, column ZORBAX SB – C18 4.6 × 15 mm). 1H NMR and ^{13}C spectra were obtained on a Varian 300 MHz spectrometer and Mercury (Varian) 400 MHz, Brooker 500 MHz, respectively. Chemical shifts given in this work are reported in ppm downfield from tetramethylsilane.

Synthesis of 5,7-disubstituted 6-aminopyrrolo[2,3-b]pyrazine-2,3-dicarbonitriles **4a–j**; **7a–j**.

Compounds **4a–j** were synthesized similarly to the method [7].

Briefly, 1.99 g (10 mmol) of compound **1** and 10 mmol of α -azaheteroarylacetonitriles **2a–e** were dissolved in 10 ml of DMF. In case of compounds **2d**, **e** the 1.01 g (10 mmol) of triethylamine was added to the reaction mixture after dissolving in DMF. After 3–4 hours of stirring at 30–40 °C, the reaction mixture was kept overnight at room temperature. The obtained precipitate was filtered, washed with little amount of DMF and acidified water, dried and recrystallized from DMF with yields 75% (**3a**); 91% (**3b**); 87% (**3c**); 95% (**3d**) and 88% (**3e**), respectively. Then, 5 mmol of either compound **3a–e** was dissolved in 5 ml DMF and 10 mmol of the appropriate amine or 3-chlorophenylhydrazine (for compound **4j**) was added by drops under stirring at room temperature. The formation of yellow precipitate was observed. The reaction mixture was kept at 50–60 °C for 2 hours, then cooled, filtered the precipitate, washed with DMF and acidified water to remove the amine

hydrochloride, dried, and recrystallized from DMF. The yields of products **4a–j** were 84–94%.

1.99 g (10 mmol) of compound **1** and 10 mmol of 2-(phenylsulfonyl)acetonitrile **5a, b** were dissolved in 6 ml of DMF. 2.02 g (20 mmol) of triethylamine was drip-added to the reaction mixture at 5 °C under stirring and cooling. After 1 hour of stirring at room temperature, the reaction mixture was mixed with 100 ml of cold water and acidified by acetic acid to neutral pH. The obtained precipitate was filtered, dried and recrystallized from dioxane with yields 81% (**6a**) and 87% (**6b**). Then, 5 mmol of either compound **6a** or **6b** was dissolved in 3 ml DMF and 5 mmol of the appropriate amine was added by drops under stirring at room temperature. The formation of precipitate was observed. The reaction mixture was kept at 50–60 °C for 2 hours, then cooled, filtered to separate the precipitate, washed with DMF and water, dried, and recrystallized from dioxane. The yields of products **7a–j** were 72–89%.

Compounds **4a–e** were synthesized as described earlier in [7].

6-Amino-5-(2-diethylamino)ethyl)-7-(1-methyl-1H-benzo[d]imidazol-2-yl)-5H-pyrrolo[3,2-b]pyrazine-2,3-dicarbonitrile (**4f**): m.p. > 300 °C; LC/MS: t_R 1.297 min (98.2%), m/z (M^+) 413.6; IR (KBr): ν_{NH_2} 3500–3200; ν_{CN} 2218; $\nu_{C=N}$ 1638 (cm^{-1}).

1H NMR (300 MHz, δ , ppm, DMSO- d_6 , J (Hz)): 9.27 (s, 2H, NH_2), 7.68 (d, 1H, Het(4)-H, $J = 6.9^*$), 7.58 (d, 1H, Het(7)-H, $J = 6.9$), 7.27 (m, 2H, Het(5,6)-H), 4.37 (t, 2H, CH_2 , $J = 5.4$), 4.00 (s, 3H, CH_3), 2.77 (t, 2H, CH_2 , $J = 5.4$), 2.52 (q, 4H, CH_2), 0.87 (t, 6H, CH_3 , $J = 6.6$).

*Het(4,5,6,7)—numbering of the benzimidazole ring.

^{13}C NMR (300 MHz, δ , ppm, DMSO- d_6): 156.9 (C_{4a}); 141.3, 140.2, 138.7 ($C_6, C_{7a}, C_{Het(2)}$); 138.1, 136.3 ($C_{Het(3a)}, C_{Het(7a)}$); 130.3, 129.0 (C_2, C_3); 116.8, 116.2 ($2C, CN$); 120.8, 119.1, 118.7, 112.1 ($C_{Het(4)}, C_{Het(5)}, C_{Het(6)}, C_{Het(7)}$); 88.6 (C_7); 57.3, 42.2, 46.9 ($4C, CH_2$); 28.9 (C, NCH_3); 11.8 ($2C, CH_3$).

5-(4-Fluorobenzyl)-6-amino-7-(1-methyl-1H-benzo[d]imidazol-2-yl)-5H-pyrrolo[3,2-b]pyrazine-2,3-dicarbonitrile (**4g**): m.p. > 300 °C; LC/MS: t_R 1.102 min (97.6%), m/z (M^+) 423.5; IR (KBr): ν_{NH_2} 3500–3200; ν_{CN} 2222; $\nu_{C=N}$ 1643 (cm^{-1}).

1H NMR (300 MHz, δ , ppm, DMSO- d_6 , J (Hz), 8.96 (s, 2H, NH_2), 7.66 (d, 1H, Het(4)-H, $J = 7.2$), 7.60 (d, 1H, Het(7)-H, $J = 7.5$), 7.37 (dd, 2H, Het(5,6)-H, $J = 4.8, J = 7.8$), 7.22 (m, 4H, Ar(2,3,5,6)-H*), 5.56 (s, 2H, CH_2), 4.03 (s, 3H, CH_3).

*Ar(2,3,4,5,6)—numbering of the phenyl substituent at position 5.

^{13}C NMR (300 MHz, δ , ppm, DMSO- d_6): 159.2 (C_{4a}); 144.8, 142.9, 140.7 ($C_6, C_{Het(2)}, C_{7a}$); 137.3 ($C_{Ar(4)}$); 135.8, 133.3 ($C_{Het(3a)}, C_{Het(7a)}$); 131.3, 128.5 (C_2, C_3); 117.0, 116.6 ($2C, CN$); 122.3, 121.2, 119.1, 118.0, 112.1, 110.4, 108.8 ($C_{Het(4)}, C_{Het(5)}, C_{Het(6)}, C_{Het(7)}, C_{Ar(1)}, C_{Ar(2)}, C_{Ar(3)}, C_{Ar(5)}, C_{Ar(6)}$); 86.8 (C_7); 41.3 (C, CH_2); 29.8 (C, NCH_3).

5-(4-Chlorobenzyl)-6-amino-7-(1-methyl-1H-benzo[d]imidazol-2-yl)-5H-pyrrolo[3,2-b]pyrazine-2,3-dicarbonitrile (**4h**): m.

p. >300 °C; LC/MS: t_R 1.143 min (99.4%), m/z (M^+) 438.9; IR (KBr): ν_{NH_2} 3500–3200; ν_{CN} 2225; $\nu_{C=N}$ 1645 (cm^{-1}).

1H NMR (300 MHz, δ , ppm, DMSO- d_6 , J (Hz)): 8.98 (s, 2H, NH_2), 7.65 (d, 1H, Het(4)-H, $J = 7.2$), 7.62 (d, 1H, Het(7)-H, $J = 6.6$), 7.43 (d, 2H, Ar(3,5)-H, $J = 8.4$), 7.32 (m, 4H, Ar(2,6)H + Het(5,6)-H), 5.56 (s, 2H, CH_2), 4.01 (3H, c, CH_3).

^{13}C NMR (300 MHz, δ , ppm, DMSO- d_6): 160.1 (C_{4a}); 145.7, 143.8, 141.6 ($C_6, C_{7a}, C_{Het(2)}$); 139.0 ($C_{Ar(4)}$); 136.7, 134.2 ($C_{Het(3a)}, C_{Het(7a)}$); 132.2, 129.4 (C_2, C_3); 116.8, 116.2 ($2C, CN$); 122.8, 122.3, 119.9, 118.7, 115.3, 112.4, 108.8 ($C_{Het(4)}, C_{Het(5)}, C_{Het(6)}, C_{Het(7)}, C_{Ar(1)}, C_{Ar(2)}, C_{Ar(3)}, C_{Ar(5)}, C_{Ar(6)}$); 84.7 (C_7); 41.8 (C, CH_2); 27.1 (C, NCH_3).

6-Amino-5-(benzo[d][1,3]dioxol-5-ylmethyl)-7-(1-methyl-1H-benzo[d]imidazol-2-yl)-5H-pyrrolo[3,2-b]pyrazine-2,3-dicarbonitrile (**4i**): m.p. > 300 °C; LC/MS: t_R 1.218 min (96.8%), m/z (M^+) 448.4; IR (KBr): ν_{NH_2} 3500–3200; ν_{CN} 2224; $\nu_{C=N}$ 1647 (cm^{-1}).

1H NMR (300 MHz, δ , ppm, DMSO- d_6 , J (Hz)): 8.96 (s, 2H, NH_2), 7.68 (d, 1H, Het(4)-H, $J = 6.6$), 7.62 (d, 1H, Het(7)-H, $J = 6.3$), 7.31 (m, 2H, Het(5,6)-H), 6.93 (m, 2H, Ar(2,6)-H), 6.87 (d, 1H, Ar(5)-H, $J = 8.4$), 6.04 (s, 2H, CH_2), 5.49 (s, 2H, CH_2), 4.03 (s, 3H, CH_3).

^{13}C NMR (300 MHz, δ , ppm, DMSO- d_6): 158.4 (C_{4a}); 148.0, 147.3 ($C_{Ar(3)}, C_{Ar(4)}$); 142.7, 140.6, 139.5 ($C_6, C_{7a}, C_{Het(2)}$); 136.1, 129.3 ($C_{Het(3a)}, C_{Het(7a)}$); 126.3, 118.0 (C_2, C_3); 116.9, 116.3 ($2C, CN$); 101.6 (C, OCH_2O); 122.3, 121.2, 118.4, 110.4, 108.8, 108.4 ($C_{Ar(1)}, C_{Ar(2)}, C_{Ar(5)}, C_{Ar(6)}, C_{Het(4)}, C_{Het(5)}, C_{Het(6)}, C_{Het(7)}$); 84.5 (C_7); 43.8 (C, CH_2); 32.7 (C, NCH_3).

6-Amino-5-(3-chlorophenylamino)-7-(1-methyl-1H-benzo[d]imidazol-2-yl)-5H-pyrrolo[3,2-b]pyrazine-2,3-dicarbonitrile (**4j**): m.p. > 300 °C; LC/MS: t_R 1.364 min (95.4%), m/z (M^+) 439.9; IR (KBr): $\nu_{NH_2, NH}$ 3500–3200; ν_{CN} 2221; $\nu_{C=N}$ 1628 (cm^{-1}).

1H NMR (300 MHz, δ , ppm, DMSO- d_6 , J (Hz)): 9.83 (s, 1H, NH); 9.01 (s, 2H, NH_2), 7.67 (d, 1H, Het(4)-H, $J = 6.9$), 7.62 (d, 1H, Het(7)-H, $J = 7.2$), 7.29 (m, 3H, Het(5,6) + Ar(5)-H), 6.99 (d, 1H, Ar(4)-H, $J = 8.4$), 6.81 (s, 1H, Ar(2)-H), 6.68 (d, 1H, Ar(6)-H, $J = 8.4$), 4.08 (s, 3H, CH_3).

^{13}C NMR (300 MHz, δ , ppm, DMSO- d_6): 162.8 (C_{4a}); 159.1 ($C_{Ar(1)}$); 147.9 ($C_{Ar(3)}$); 142.8, 139.6, 138.7 ($C_6, C_{7a}, C_{Het(2)}$); 136.2, 134.4 ($C_{Het(3a)}, C_{Het(7a)}$); 127.1, 117.9 (C_2, C_3); 116.6, 116.1 ($2C, CN$); 131.4, 122.4, 121.0, 118.5, 112.8, 111.9, 110.5 ($C_{Ar(2)}, C_{Ar(4)}, C_{Ar(5)}, C_{Ar(6)}, C_{Het(4)}, C_{Het(5)}, C_{Het(6)}, C_{Het(7)}$); 82.8 (C_7); 36.2 (C, NCH_3).

5-Chloro-6-[cyano(phenylsulfonyl)methyl]-2,3-pyrazinedicarbonitrile N-triethylammonium salt (**6a**): m.p. 158–159 °C; LC/MS: t_R 0.973 min (100.0%), m/z (M^+) 343.6; IR (KBr): ν_{CN} 2195, 2227; $\nu_{C=N}$ 1645; ν_{SO_2} 1290(as), 1135(s) (cm^{-1}).

1H NMR (300 MHz, δ , ppm, DMSO- d_6 , J (Hz)): 10.74 (S_{broad} , 1H, N^+H), 7.86 (m, 2H, Ar(2',6')-H*), 7.55 (m, 3H, Ar(3',4',5')-H), 3.09 (m, 6H, CH_2), 1.17 (t, 9H, CH_3 , $J = 9$).

^{13}C NMR (300 MHz, δ , ppm, DMSO- d_6): 151.9 (C_2); 143.9 (C_3); 139.4 (C_6); 132.5 ($C_{Ar(4)}$); 129.7 ($C_{Ar(1)}$); 128.7, 127.9 ($C_{Ar(2)}$, $C_{Ar(3)}$, $C_{Ar(5)}$, $C_{Ar(6)}$); 118.5 (C_5); 116.0, 115.3, 114.1 ($3C, CN$); 79.6 (C_C); 46.3 ($3C, CH_2$); 9.1 ($3C, CH_3$).

* Ar(2',3',4',5',6')—numbering of the phenylsulfonyl substituent at position 7.

5-Chloro-6-[[[4-chlorophenylsulfonyl](cyano)methyl]-2,3-pyrazinedicarbonitrile N-triethylammonium salt (**6b**): m.p. 159–160 °C; LC/MS: t_R 1.054 min (98.4%), m/z (M^+) 379.6; IR (KBr): ν_{CN} 2185, 2225; $\nu_{C=N}$ 1640; ν_{SO_2} 1289(as), 1138(s) (cm^{-1}).

1H NMR (300 MHz, δ , ppm, DMSO- d_6 , J (Hz)): 11.20 (S_{broad} , 1H, N^+H), 7.85 (d, 2H, Ph(2',6')-H, $J = 9$), 7.61 (d, 2H, Ar(3',5')-H, $J = 9$), 3.10 (m, 6H, CH_2), 1.18 (t, 9H, CH_3 , $J = 9$).

^{13}C NMR (300 MHz, δ , ppm, DMSO- d_6): 151.9 (C_2); 142.8 (C_3); 139.6 (C_6); 137.3 ($C_{Ar(4')}$); 129.7 ($C_{Ar(1')}$); 129.8, 128.8 ($C_{2Ar'}$, $C_{3Ar'}$, $C_{5Ar'}$, $C_{6Ar'}$); 118.3 (C_5); 116.4, 115.2, 114.1 (3C CN); 79.0 (C_C); 46.3 (3C, CH_2); 9.1 (3C, CH_3).

6-Amino-5-phenethyl-7-(phenylsulfonyl)-5H-pyrrolo[3,2-b]pyrazine-2,3-dicarbonitrile (**7a**): m.p. > 300 °C; LC/MS: t_R 1.121 min (99.8%), m/z (M^+) 429.6; IR (KBr): ν_{NH_2} 3398(as), 3308(s); ν_{CN} 2210; $\nu_{C=N}$ 1648; ν_{SO_2} 1297(as), 1150(s) (cm^{-1}).

1H NMR (300 MHz, δ , ppm, DMSO- d_6 , J (Hz)): 8.69 (s, 2H, NH_2), 8.02 (d, 2H, Ar(2,6)-H, $J = 7.8$), 7.67 (m, 3H, Ar(3,4,5)-H), 7.07 (m, 5H, Ar-H), 4.41 (t, 2H, CH_2 , $J = 7.5$), 2.93 (t, 2H, CH_2 , $J = 7.5$).

^{13}C NMR (300 MHz, δ , ppm, DMSO- d_6): 155.4 (C_{4a}); 143.3, 141.6, 140.5 (C_6 , C_{7a} , $C_{Ar(1')}$); 126.7, 121.3 (C_2 , C_3); 116.1 (2C, CN); 133.6, 130.7, 126.2, 122.3, 121.2, 118.4, 118.0, 110.4, 108.8 ($C_{Ar(1)}$, $C_{Ar(2)}$, $C_{Ar(3)}$, $C_{Ar(4)}$, $C_{Ar(5)}$, $C_{Ar(6)}$, $C_{Ar(2')}$, $C_{Ar(3')}$, $C_{Ar(4')}$, $C_{Ar(5')}$, $C_{Ar(6')}$), 89.5 (C_7); 47.2 (2C, CH_2).

6-Amino-5-(2-diethylamino)ethyl-7-(phenylsulfonyl)-5H-pyrrolo[3,2-b]pyrazine-2,3-dicarbonitrile (**7b**): m.p. > 300 °C; LC/MS: t_R 1.176 min (98.7%), m/z (M^+) 424.5; IR (KBr): ν_{NH_2} 3404(as), 3323(s); ν_{CN} 2224; $\nu_{C=N}$ 1642; ν_{SO_2} 1303(as), 1140 (s) (cm^{-1}).

1H NMR (300 MHz, δ , ppm, DMSO- d_6 , J (Hz)): 8.90 (s, 2H, NH_2), 8.04 (d, 2H, Ar(2',6')-H, $J = 2.1$), 7.65 (m, 3H, Ar(3',4',5')-H), 4.25 (t, 2H, CH_2 , $J = 4.8$), 2.66 (t, 2H, CH_2 , $J = 4.8$), 2.41 (qr, 4H, CH_2 , $J = 6.9$), 0.74 (t, 6H, CH_3 , $J = 6.9$).

^{13}C NMR (300 MHz, δ , ppm, DMSO- d_6): 156.9 (C_{4a}), 143.1, 141.0, 140.0 (C_6 , C_{7a} , $C_{Ar(1')}$); 125.9, 120.5 (C_2 , C_3); 115.5 (2C, CN); 133.2, 129.3, 125.8 ($C_{Ar(2')}$, $C_{Ar(3')}$, $C_{Ar(4')}$, $C_{Ar(5')}$, $C_{Ar(6')}$), 90.4 (C_7), 50.43 (2C, NCH_2CH_3), 46.3 (2C, NCH_2CH_2N), 11.5 (2C, CH_3).

6-Amino-5-(4-methylbenzyl)-7-(phenylsulfonyl)-5H-pyrrolo[3,2-b]pyrazine-2,3-dicarbonitrile (**7c**): m.p. > 300 °C; LC/MS: t_R 1.169 min (96.3%), m/z (M^+) 429.5; IR (KBr): ν_{NH_2} 3398(as), 3324(s); ν_{CN} 2227; $\nu_{C=N}$ 1643; ν_{SO_2} 1285(as), 1135(s) (cm^{-1}).

1H NMR (300 MHz, δ , ppm, DMSO- d_6 , J (Hz)): 8.73 (s, 2H, NH_2), 8.08 (d, 2H, Ar(2,6)-H, $J = 6.6$), 7.33 (m, 3H, Ar(3,4,5)-H), 7.13 (d, 2H, Ar(3',5')-H, $J = 8.1$), 7.11 (d, 2H, Ar(2',6')-H, $J = 8.1$), 5.39 (s, 2H, CH_2), 2.52 (s, 3H, CH_3).

^{13}C NMR (300 MHz, δ , ppm, DMSO- d_6): 157.3 (C_{4a}); 143.1, 140.7, 140.1 (C_6 , C_{7a} , $C_{Ar(1')}$); 126.9, 121.5 (C_2 , C_3); 134.5, 133.8, 129.9, 128.7, 126.4, 122.6, 120.0, 120.2, 108.8, 108.3 ($C_{Ar(1)}$, $C_{Ar(2)}$, $C_{Ar(3)}$, $C_{Ar(4)}$, $C_{Ar(5)}$, $C_{Ar(6)}$, $C_{Ar(2')}$,

$C_{Ar(3')}$, $C_{Ar(4')}$, $C_{Ar(5')}$, $C_{Ar(6')}$); 116.1, 115.8 (2C, CN); 87.4 (C_7); 43.8 (C, CH_2); 21.5 (C, CH_3).

6-Amino-5-(4-chlorobenzyl)-7-(phenylsulfonyl)-5H-pyrrolo[3,2-b]pyrazine-2,3-dicarbonitrile (**7d**): m.p. > 300 °C; LC/MS: t_R 1.186 min (97.7%), m/z (M^+) 449.9; IR (KBr): ν_{NH_2} 3392(as), 3308(s); ν_{CN} 2218; $\nu_{C=N}$ 1633; ν_{SO_2} 1308(as), 1146(s) (cm^{-1}).

1H NMR (300 MHz, δ , ppm, DMSO- d_6 , J (Hz)): 8.56 (s, 2H, NH_2), 8.18 (d, 2H, Ar(2,6)-H, $J = 6.6$), 7.45 (m, 3H, Ar(3,4,5)-H), 7.17 (d, 2H, Ar(3',5')-H, $J = 7.9$), 7.06 (d, 2H, Ar(2',6')-H, $J = 7.9$), 5.29 (s, 2H, CH_2).

^{13}C NMR (300 MHz, δ , ppm, DMSO- d_6): 158.4 (C_{4a}); 142.7, 140.6, 139.5 (C_6 , C_{7a} , $C_{Ar(1')}$); 136.1 ($C_{Ar(4)}$); 129.3, 126.3 (C_2 , C_3); 116.9, 116.3 (2C, CN); 148.0, 147.3, 122.3, 121.2, 118.4, 118.0, 110.4, 108.8, 108.4 ($C_{Ar(1)}$, $C_{Ar(2)}$, $C_{Ar(3)}$, $C_{Ar(5)}$, $C_{Ar(6)}$, $C_{Ar(2')}$, $C_{Ar(3')}$, $C_{Ar(4')}$, $C_{Ar(5')}$, $C_{Ar(6')}$); 84.5 (C_7); 43.8 (C, CH_2).

6-Amino-5-(4-methoxybenzyl)-7-(phenylsulfonyl)-5H-pyrrolo[3,2-b]pyrazine-2,3-dicarbonitrile (**7e**): m.p. > 300 °C; LC/MS: t_R 1.256 min (95.9%), m/z (M^+) 445.7; IR (KBr): ν_{NH_2} 3400(as), 3315(s); ν_{CN} 2221; $\nu_{C=N}$ 1628; ν_{SO_2} 1270(as), 1080 (s) (cm^{-1}).

1H NMR (300 MHz, δ , ppm, DMSO- d_6 , J (Hz)): 8.75 (s, 2H, NH_2), 8.12 (d, 2H, Ar(2,6)-H, $J = 6.3$), 7.72 (m, 3H, Ar(3,4,5)-H), 7.23 (d, 2H, Ar(3',5')-H, $J = 8.4$), 6.97 (d, 2H, Ar(2',6')-H, $J = 8.4$), 5.43 (s, 2H, CH_2), 3.78 (s, 3H, OCH_3).

^{13}C NMR (300 MHz, δ , ppm, DMSO- d_6): 160.0 (C_{4Ar}); 157.5 (C_{4a}); 142.2, 140.6, 140.1 (C_6 , C_{7a} , $C_{Ar(1')}$); 126.5, 121.6 (C_2 , C_3); 133.9, 132.8, 127.9, 127.7, 125.2, 121.1, 120.7, 120.2, 108.0, 107.3 ($C_{Ar(1)}$, $C_{Ar(2)}$, $C_{Ar(3)}$, $C_{Ar(5)}$, $C_{Ar(6)}$, $C_{Ar(2')}$, $C_{Ar(3')}$, $C_{Ar(4')}$, $C_{Ar(5')}$, $C_{Ar(6')}$); 116.2, 115.7 (2C, CN); 85.5 (C_7); 64.8 (C, OCH_3); 42.2 (C, CH_2).

6-Amino-5-(benzo[d][1,3]dioxol-5-ylmethyl)-7-(phenylsulfonyl)-5H-pyrrolo[3,2-b]pyrazine-2,3-dicarbonitrile (**7f**): m.p. > 300 °C; LC/MS: t_R 1.198 min (97.6%), m/z (M^+) 459.5; IR (KBr): ν_{NH_2} 3379(as), 3304(s); ν_{CN} 2230; $\nu_{C=N}$ 1649; ν_{SO_2} 1303(as), 1141(s) (cm^{-1}).

1H NMR (300 MHz, δ , ppm, DMSO- d_6 , J (Hz)): 8.66 (s, 2H, NH_2), 8.06 (d, 2H, Ar(2,6)-H, $J = 6.3$), 7.65 (m, 3H, Ar(3,4,5)-H), 6.86 (m, 2H, Ar(5',6')-H), 6.76 (d, 1H, Ar(2')-H, $J = 8.1$), 5.99 (s, 2H, CH_2), 5.33 (s, 2H, CH_2).

^{13}C NMR (300 MHz, δ , ppm, DMSO- d_6): 156.2 (C_{4a}); 147.9, 147.3 ($C_{Ar(3)}$, $C_{Ar(4)}$); 143.4, 140.8, 140.5 (C_6 , C_{7a} , $C_{Ar(1')}$); 126.9, 121.5 (C_2 , C_3); 134.5 ($C_{Ar(1)}$); 133.8, 129.9, 126.4 ($C_{Ar(2')}$, $C_{Ar(3')}$, $C_{Ar(4')}$, $C_{Ar(5')}$, $C_{Ar(6')}$); 121.2 ($C_{Ar(6)}$); 116.1 (2C, CN); 108.8, 108.3 ($C_{Ar(2)}$, $C_{Ar(5)}$); 101.6 (C, OCH_2O); 90.9 (C_7); 43.8 (C, NCH_2Ph).

6-Amino-5-(4-ethoxyphenyl)-7-(phenylsulfonyl)-5H-pyrrolo[3,2-b]pyrazine-2,3-dicarbonitrile (**7g**): m.p. > 300 °C; LC/MS: t_R 1.168 min (96.2%), m/z (M^+) 445.6; IR (KBr): ν_{NH_2} 3392(as), 3308(s); ν_{CN} 2218; $\nu_{C=N}$ 1633; ν_{SO_2} 1308(as), 1146 (s) (cm^{-1}).

1H NMR (300 MHz, δ , ppm, DMSO- d_6 , J (Hz)): 8.21 (s, 2H, NH_2), 8.06 (dd, 2H, Ar(2,6)-H, $J = 7.8$, $J = 1.5$), 7.68 (m, 3H, Ar(3,4,5)-H), 7.43 (d, 2H, Ar(3,5)-H, $J = 9$), 7.17 (d, 2H, Ar(2,6)-H, $J = 9$), 4.12 (qr, 2H, CH_2 , $J = 6.9$), 1.39 (t, 3H, CH_3 , $J = 6.9$).

^{13}C NMR (300 MHz, δ , ppm, DMSO- d_6): 160.3 (C, COC_2H_5); 158.4 (C_{4a}); 143.4, 142.2, 140.7 (C_6 , C_{7a} , $\text{C}_{\text{Ar}(1)}$); 133.8 ($\text{C}_{\text{Ar}(1)}$), 122.8, 121.4 (C_2 , C_3); 116.0 (2C, CN); 130.6, 129.9, 126.6, 116.1 ($\text{C}_{\text{Ar}(2)}$, $\text{C}_{\text{Ar}(3)}$, $\text{C}_{\text{Ar}(5)}$, $\text{C}_{\text{Ar}(6)}$, $\text{C}_{\text{Ar}(2)}$, $\text{C}_{\text{Ar}(3)}$, $\text{C}_{\text{Ar}(4)}$, $\text{C}_{\text{Ar}(5)}$, $\text{C}_{\text{Ar}(6)}$); 90.7 (C_7); 64.0 (C, OCH_2); 15.1 (C, CH_3).

6-Amino-5-(3,4-dimethoxyphenethyl)-7-(4-chlorophenylsulfonyl)-5H-pyrrolo[3,2-b]pyrazine-2,3-dicarbonitrile (**7h**): m.p. > 300 °C; LC/MS: t_R 1.247 min (98.6%), m/z (M^+) 524.0; IR (KBr): ν_{NH_2} 3403(as), 3319(s); ν_{CN} 2215; $\nu_{\text{C=N}}$ 1638; ν_{SO_2} 1305(as), 1135(s) (cm^{-1}).

^1H NMR (300 MHz, δ , ppm, DMSO- d_6 , J (Hz)): 8.68 (s, 2H, NH_2), 8.02 (d, 2H, $\text{Ar}(2,6)\text{-H}$, $J = 9$), 7.76 (d, 2H, $\text{Ar}(3,5)\text{-H}$, $J = 8.7$), 6.66 (s, 1H, $\text{Ar}(2')\text{-H}$), 6.57 (d, 1H, $\text{Ar}(5')\text{-H}$, $J = 6$), 6.52 (d, 1H, $\text{Ar}(6')\text{-H}$, $J = 6$), 4.40 (t, 2H, CH_2 , $J = 6.8$), 3.87 (t, 2H, CH_2 , $J = 6.8$), 3.66 (s, 3H, OCH_3), 3.59 (s, 3H, OCH_3).

^{13}C NMR (300 MHz, δ , ppm, DMSO- d_6): 157.4(C_{4a}); 146.8, 145.3 ($\text{C}_{\text{Ar}(3)}$, $\text{C}_{\text{Ar}(4)}$); 143.1, 141.0, 140.7 (C_6 , C_{7a} , $\text{C}_{\text{Ar}(1)}$); 136.5 ($\text{C}_{\text{Ar}(4)}$); 126.6, 121.2 (C_2 , C_3); 116.4, 116.1 (2C, CN); 133.6, 130.4, 126.7, 124.3, 121.2, 118.0, 111.1, 108.3 ($\text{C}_{\text{Ar}(1)}$, $\text{C}_{\text{Ar}(2)}$, $\text{C}_{\text{Ar}(5)}$, $\text{C}_{\text{Ar}(6)}$, $\text{C}_{\text{Ar}(2)}$, $\text{C}_{\text{Ar}(3)}$, $\text{C}_{\text{Ar}(5)}$, $\text{C}_{\text{Ar}(6)}$); 82.2 (C_7); 65.8, 58.3 (2C, OCH_3); 44.2, 38.7 (2C, CH_2).

6-Amino-5-phenethyl-7-(4-chlorophenylsulfonyl)-5H-pyrrolo[3,2-b]pyrazine-2,3-dicarbonitrile (**7i**): m.p. > 300 °C; LC/MS: t_R 1.187 min (97.9%), m/z (M^+) 463.2; IR (KBr): ν_{NH_2} 3396(as), 3322(s); ν_{CN} 2226; $\nu_{\text{C=N}}$ 1643; ν_{SO_2} 1308(as), 1141 (s) (cm^{-1}).

^1H NMR (300 MHz, δ , ppm, DMSO- d_6 , J (Hz)): 8.72 (s, 2H, NH_2), 8.03 (d, 2H, $\text{Ar}(2,6)\text{-H}$, $J = 8.7$), 7.78 (d, 2H, $\text{Ar}(3,5)\text{-H}$, $J = 8.7$), 7.15 (m, 5H, Ph-H), 4.23 (t, 2H, CH_2 , $J = 6.8$), 2.96 (t, 2H, CH_2 , $J = 6.8$).

^{13}C NMR (300 MHz, δ , ppm, DMSO- d_6): 157.3(C_{4a}); 143.3, 141.5, 140.4 (C_6 , C_{7a} , $\text{C}_{\text{Ar}(1)}$); 135.8 ($\text{C}_{\text{Ar}(4)}$); 126.2, 121.0 (C_2 , C_3); 116.3, 116.1 (2C, CN); 130.7, 128.4, 126.2, 122.3, 121.2, 118.4, 118.0, 110.4, 108.8 ($\text{C}_{\text{Ar}(1)}$, $\text{C}_{\text{Ar}(2)}$, $\text{C}_{\text{Ar}(3)}$, $\text{C}_{\text{Ar}(4)}$, $\text{C}_{\text{Ar}(5)}$, $\text{C}_{\text{Ar}(6)}$, $\text{C}_{\text{Ar}(2)}$, $\text{C}_{\text{Ar}(3)}$, $\text{C}_{\text{Ar}(5)}$, $\text{C}_{\text{Ar}(6)}$), 83.2 (C_7); 44.6, 37.9 (2C, CH_2).

6-Amino-5-(4-methoxybenzyl)-7-(4-chlorophenylsulfonyl)-5H-pyrrolo[3,2-b]pyrazine-2,3-dicarbonitrile (**7j**): m.p. > 300 °C;

LC/MS: t_R 1.47 min (98.4%), m/z (M^+) 489.1; IR (KBr): ν_{NH_2} 3395(as), 3307(s); ν_{CN} 2220; $\nu_{\text{C=N}}$ 1640; ν_{SO_2} 1303(as), 1145(s) (cm^{-1}).

^1H NMR (300 MHz, δ , ppm, DMSO- d_6 , J (Hz)): 8.74 (s, 2H, NH_2), 8.07 (d, 2H, $\text{Ar}(2,6)\text{-H}$, $J = 8.4$), 7.75 (d, 2H, $\text{Ar}(3,5)\text{-H}$, $J = 8.4$), 7.21 (d, 2H, $\text{Ar}(3',5')\text{-H}$, $J = 8.7$), 6.93 (d,

2H, $\text{Ar}(2',6')\text{-H}$, $J = 8.7$), 5.38 (s, 2H, CH_2), 3.74 (s, 3H, OCH_3).

^{13}C NMR (300 MHz, δ , ppm, DMSO- d_6): 159.3 ($\text{C}_{\text{Ar}(4)}$); 154.7 (C_{4a}); 142.6, 140.2, 139.6 (C_6 , C_{7a} , $\text{C}_{\text{Ar}(1)}$); 136.4 ($\text{C}_{\text{Ar}(4)}$); 126.2, 121.2 (C_2 , C_3); 133.7, 132.3, 127.0, 125.8, 121.6, 120.8, 108.0, 107.3 ($\text{C}_{\text{Ar}(1)}$, $\text{C}_{\text{Ar}(2)}$, $\text{C}_{\text{Ar}(3)}$, $\text{C}_{\text{Ar}(5)}$, $\text{C}_{\text{Ar}(6)}$, $\text{C}_{\text{Ar}(2)}$, $\text{C}_{\text{Ar}(3)}$, $\text{C}_{\text{Ar}(5)}$, $\text{C}_{\text{Ar}(6)}$); 116.1, 115.9 (2C, CN); 88.3 (C_7); 66.1 (C, OCH_3); 48.6 (C, CH_2).

All synthesized compounds are commercially available from Enamine Ltd. DataBase (www.enamine.net).

Acknowledgments

The authors are grateful to the colleagues at National Cancer Institute (USA) who participated in Developmental Therapeutics Program, to Enamine Ltd. (www.enamine.net) for financial support, and to Dr. A. Shtil for critical review of the manuscript.

References

- [1] C. Sablayrolles, G.H. Cros, J.C. Milhavet, E. Rechenq, J.P. Chapat, M. Boucard, J.J. Serrano, J.H. McNeill, *J. Med. Chem.* 27 (1984) 206–212.
- [2] A. Trejo, H. Arzeno, M. Browner, S. Chanda, S. Cheng, D.D. Comer, et al., *J. Med. Chem.* 46 (2003) 4702–4713.
- [3] P. Ge, T. Kalman, *Bioorg. Med. Chem. Lett.* 23 (1997) 3023–3026.
- [4] Y. Mettey, M. Gompel, V. Thomas, M. Garnier, M. Leost, I. Ceballos-Picot, et al., *J. Med. Chem.* 46 (2003) 222–236.
- [5] L. Meijer, M. Flajolet, *Trends Pharmacol. Sci.* 25 (2004) 471–480.
- [6] M. Mapelli, L. Massimilino, C. Crovace, M.A. Seeliger, L.-H. Tsai, L. Meijer, A. Musacchio, *J. Med. Chem.* 48 (2005) 671–679.
- [7] Y.M. Volovenko, G.G. Dubinina, *Chemistry of Heterocyclic Compounds* 3 (2002) 372–379.
- [8] Y.M. Volovenko, G.G. Dubinina, *Chemistry of Heterocyclic Compounds* 2 (2002) 241–247.
- [9] G.L. Warren, W. Andrews, A.-M. Capelli, B. Clarke, J. LaLonde, M.H. Lambert, et al., *J. Med. Chem.* (2005) ASAP article; doi: 10.1021/jm050362n.
- [10] L. Meijer, A.-L. Skaltsounis, P. Magiatis, P. Polychronopoulos, M. Knockaert, M. Leost, et al., *Chem. Biol.* 10 (2003) 1255–1264.
- [11] A.M. Lawrie, M.E. Noble, P. Tunnah, N.R. Brown, L.N. Johnson, J.A. Endicott, *Nat. Struct. Biol.* 4 (1997) 796–799.
- [12] J. Stamos, M.X. Sliwowski, C. Eigenbrot, *J. Biol. Chem.* 277 (2002) 46265–46272.
- [13] M. Knockaert, P. Greengard, L. Meijer, *Trends Pharmacol. Sci.* 23 (2002) 417–425.
- [14] R. Perez-Soler, *Oncologist* 9 (2004) 58–67.
- [15] R.D. Mass, *Int. J. Radiat. Oncol. Biol. Phys.* 58 (2004) 932–940.
- [16] J.F. Lowrie, R.K. Delisle, D.W. Hobbs, D.J. Diller, *Comb. Chem. High Throughput Screen.* 7 (2004) 495–510.
- [17] C. McMartin, R.S. Bohacek, *J. Comput. Aided Mol. Des.* 11 (1997) 333–344.